


Nonlinear phase bores in drift wave-zonal flow dynamics

Cite as: Phys. Plasmas **26**, 102304 (2019); <https://doi.org/10.1063/1.5111987>

Submitted: 31 May 2019 . Accepted: 22 September 2019 . Published Online: 10 October 2019

H. Kang , and P. H. Diamond 



View Online



Export Citation



CrossMark



NEW

AVS Quantum Science

A high impact interdisciplinary journal for **ALL** quantum science

ACCEPTING SUBMISSIONS

Nonlinear phase bores in drift wave-zonal flow dynamics

Cite as: Phys. Plasmas **26**, 102304 (2019); doi: [10.1063/1.5111987](https://doi.org/10.1063/1.5111987)

Submitted: 31 May 2019 · Accepted: 22 September 2019 ·

Published Online: 10 October 2019



View Online



Export Citation



CrossMark

H. Kang^{a)} and P. H. Diamond

AFFILIATIONS

Department of Physics, University of California, San Diego, California 92093, USA

^{a)}Present address: Department of Physics, University of Maryland, College Park, MD 20742, USA.

ABSTRACT

A minimal model of nonlinear phase dynamics in drift waves is shown to support phase bore solutions. Coupled nonlinear equations for amplitude, phase, and zonal flow are derived for the Hasegawa-Mima system and specialized to the case of spatiotemporally constant amplitude. In that limit, phase curvature (finite second derivative of the phase with respect to the radius) alone generates propagating shear flows. The phase field evolves nonlinearly by a competition between phase steepening and dispersion. The analytical solution of the model reveals that the phase bore solutions so obtained realize the concept of a phase slip in a concrete dynamical model of drift wave dynamics. The implications for phase turbulence are discussed.

Published under license by AIP Publishing. <https://doi.org/10.1063/1.5111987>

I. INTRODUCTION

Anomalous transport and its prediction continue to be foci of interest in plasma and fusion theory. The central theoretical problem related to turbulent transport is the calculation of the fluxes, such as $\langle \tilde{v}_r \tilde{n} \rangle$, $\langle \tilde{v}_r \tilde{T} \rangle$, $\langle \tilde{v}_r \tilde{v}_\phi \rangle$, etc. Fluxes are determined by fluctuation intensities, such as $\langle \tilde{v}_r^2 \rangle$, $\langle \tilde{n}^2 \rangle$, $\langle \tilde{T}^2 \rangle$, etc., and, notably, the “cross-phase” between the fluctuations which determine the flux. Here, if the particle flux is $\Gamma = \langle \tilde{v}_r \tilde{n} \rangle$, the relevant cross phase is given by $\cos \theta = \langle \tilde{v}_r \tilde{n} \rangle / \langle \tilde{v}_r^2 \rangle^{1/2} \langle \tilde{n}^2 \rangle^{1/2}$, i.e., the cosine of the angle between the radial velocity fluctuation and the density fluctuation. The flux is set by a product of three elements, namely, two rms fluctuation levels (here $\langle \tilde{v}_r^2 \rangle^{1/2}$, $\langle \tilde{n}^2 \rangle^{1/2}$) and the cross phase. We note in passing that even if individual fluctuations follow a Gaussian probability-distribution, the flux can exhibit a non-Gaussian tail.

Of course, the dynamic relation of fluxes to fluctuation intensities has been studied intensively and discussed in hundreds, if not thousands, of papers.¹ However, the actual “dynamics” of the cross-phase has received considerably less attention. Usually, the cross-phase is taken as set by the ratio of the spectral autocorrelation rate (i.e., for quasilinear analyses) or the response decorrelation rate (i.e., for nonlinear analyses) to the frequency.² A few studies at least allow for a change in the cross-phase at a transport bifurcation—say, as a result of the effect of strong $\mathbf{E} \times \mathbf{B}$ shear on the autocorrelation time.³ In general, however, the cross-phase is treated as a prescribed function of plasma parameters.

Recently, however, there is increasing awareness that the phase adjusts “dynamically” and thus must be treated as evolving in time on mesoscopic, and even microscopic, time scales.⁴ Such a time dependence can profoundly affect transport. In addition, the cross-phase may be spatially multiscale and so manifest a mesoscopic envelope structure. Both of these phase dependencies are neglected in quasilinear theory or simple nonlinear models, such as resonance broadening theory.⁵ These observations point to a need to consider the role of “phase dynamics” in turbulent transport and fluctuation evolution.⁶ Note that phase dynamics has long been a central element of pattern formation theory.⁷ One example of an approach to flow pattern formation is that of D. Y. Manin,⁸ which utilized a hodographic technique to formulate the coupling of waves and vortices. Pattern formation in drift wave-zonal flow turbulence is reviewed in Refs. 9 and 11.

One time dependent phenomenon in phase dynamics is the “phase slip,” i.e., an abrupt jump in the phase which occurs between longer time periods of constant phase. Phase slips occur in systems governed by the Adler equation,⁹ the general form of which may be written as

$$\frac{d}{dt} \Delta\phi = -(\omega - \omega_0) + \varepsilon q(\Delta\phi).$$

Here, $\Delta\phi = \phi - \omega t$ is the difference between the phases of the forcing and the oscillation. Depending on q , the phases can either lock or slip and so assume very different values, with (possibly very) different implications for the transport flux. One concrete realization of the

Adler equation structure in a fusion-related problem was suggested in Ref. 4, which addressed phase dynamics of ballooning modes in the context of a 0D model of edge-localized modes (ELMs). There, ω_0 was the (prescribed) $\mathbf{E} \times \mathbf{B}$ shearing frequency and $q(\Delta\phi)$ was related to the transport flux. The upshot was that the phase would hover for long periods at a value which gave zero transport, but jump or slip during short intervals, during which transport occurred and profiles relaxed. Thus, transport is determined by phase evolution on multiple time scales. The discussion above motivates our desire to deeply understand the evolution and dynamics of cross-phase in drift wave-zonal flow turbulence,¹⁰ in the context of a minimal model containing the relevant physics. The goal here is to understand what types of spatiotemporal phase structures and/or solutions are manifested in the system. A model which is more realistic than that of Ref. 4 is required. To isolate phase dynamics, a simplifying restriction of spatiotemporally constant mode amplitude is imposed. In this limit, the requisite Reynolds force for zonal flow generation is produced by the “phase curvature,”¹¹ i.e.,

$$-\partial_x \langle \tilde{v}_r \tilde{v}_\theta \rangle \simeq \sum_{k_y} |A_{k_y}|^2 k_y \partial_x^2 \psi_{k_y} \simeq |A|^2 \sum_{k_y} k_y \partial_x^2 \psi_{k_y}.$$

Thus, the system can be reduced to 1D equations for the space-time evolution of the phases and flow. Note how phase curvature is simply the second derivative of the phase ψ with respect to x , i.e., $\partial_x^2 \psi_{k_x}$. It does not refer to the Gaussian curvature. The finite phase curvature here is equivalent to a spatially varying radial wavenumber, $\partial_x k_x \neq 0$.

In this paper, we analyze a minimal model of phase dynamics of the drift wave-zonal flow system. Coupled nonlinear equations for amplitude, phase, and zonal flow field are derived for the Hasegawa-Mima system.¹² The phase is treated on equal footing with the other fields. In order to focus on phase dynamics, we consider only the case of spatiotemporally constant amplitude. We show that energy is conserved between flow and fluctuations in this limit. Phase curvature ($\partial_x k_x \neq 0$) sets the Reynolds force. The coupled phase and flow system generates propagating solutions, i.e., of the form $\langle v_y(x, t) \rangle = \langle v_y(x - ct) \rangle$. The associated phase field evolves nonlinearly by a competition between phase steepening and dispersion, much as a collisionless shock or soliton does.¹³ Explicit analytical solutions for the system are obtained. The propagating shear layer is accompanied by a propagating “phase bore” structure (see Fig. 2). This realizes the concept of a phase slip (motivated by the simple and generic Adler equation) in a concrete dynamical model of drift wave-zonal flow turbulence. In particular, we see that the phase slip appears as a propagating space-time structure—a bore. The implications for a state of phase turbulence are discussed. We note that an ensemble of phase slips should exist in turbulence and lead to stochastic variation of the frequency and the associated flux (through its effect on $\omega - \omega_c^*$).

The remainder of this paper is organized as follows. Section II gives the model and basic system of equations. In Sec. III, the physics of phase and flow evolution are discussed. Phase bore or slip and shear layer solutions are presented in Sec. IV. Section V presents conclusions and discussion.

II. MODEL AND SYSTEM OF EQUATIONS

We consider drift wave evolution using the minimal model—the Hasegawa-Mima equation—with self-consistent zonal shear flow,^{14,15}

$$0 = \partial_t (\tilde{\phi} - \rho_s^2 \nabla^2 \tilde{\phi}) + v^* \partial_y \tilde{\phi} + \bar{\mathbf{v}}_E \cdot \nabla (\tilde{\phi} - \rho_s^2 \nabla^2 \tilde{\phi}) - \bar{\mathbf{v}}_E \cdot \nabla (\rho_s^2 \nabla^2 \tilde{\phi}) + \tilde{\mathbf{v}}_E \cdot \nabla (\tilde{\phi} - \rho_s^2 \nabla^2 \tilde{\phi}). \quad (1)$$

Here, $\rho_s^2 = T_e / (m_i \Omega_i^2)$, $v^* = \rho_s^2 \Omega_i / L_n$, where $L_n = -(d_x n_0 / n_0)^{-1}$, and $\bar{\mathbf{v}}_E = \rho_s^2 \Omega_i \hat{\mathbf{z}} \times \nabla \phi$, which is the $\mathbf{E} \times \mathbf{B}$ drift with \mathbf{B} pointing in $\hat{\mathbf{z}}$, i.e., the axial or toroidal direction. Both the flow and the electrostatic potential field ϕ have been separated into their respective microscale fluctuations ($\tilde{\cdot}$) and mesoscale mean ($\bar{\cdot}$). Since we approach the problem through mean field theory, the last term on the right hand side of Eq. (1), representing fluctuation nonlinearity, is dropped hereafter.

The evolution of the zonal flow ($k_\theta = 0, k_z = 0$) is described in 2D by

$$\partial_t \langle v_y \rangle = \rho_s^4 \Omega_i^2 \partial_x \langle \partial_y \tilde{\phi} \partial_x \tilde{\phi} \rangle - \mu \langle v_y \rangle, \quad (2)$$

where $\langle v_y(x) \rangle \equiv \bar{\mathbf{v}}_E \cdot \hat{\mathbf{y}}$ is the velocity of the zonal flow (averaged in the poloidal direction), $\langle \partial_y \tilde{\phi} \partial_x \tilde{\phi} \rangle$ is the Reynolds stress, $\hat{\mathbf{x}}$ represents the radial direction, and μ is the drag damping coefficient. Here, drag (usually associated with toroidal effects) is inserted *ad hoc* into an otherwise slab model. The purpose of the drag is to provide a scale-independent damping, which limits flow evolution on large scales.

To systematically investigate the role of dynamic phase evolution in the DW-ZF system, we write the DW fluctuation as $\tilde{\phi} = A(x, y, t) e^{i\psi(x, y, t)}$, where $\psi(x, y, t)$ is the phase of the drift wave and $A(x, y, t)$ is the amplitude. As both the amplitude and phase are real, we separate the real and imaginary parts of Eq. (1), which gives the amplitude equation

$$0 = \partial_t A + (2\nabla A \cdot \nabla \psi + A \nabla^2 \psi) \hat{\chi}(A) + (\nabla \psi)^2 \hat{\chi}(A) - \hat{\chi}(\nabla^2 A) + 2A \nabla \psi \cdot \hat{\chi}(\nabla \psi) + \langle v_y \rangle \partial_y A + \rho_s^2 \langle v_y \rangle'' \partial_y A + v^* \partial_y A \quad (3)$$

and the phase equation

$$0 = A \partial_t \psi - 2 \nabla \psi \cdot \hat{\chi}(\nabla A) - 2 \nabla A \cdot \hat{\chi}(\nabla \psi) - (\nabla^2 A - A(\nabla \psi)^2) \hat{\chi}(\psi) - \nabla^2 \psi \hat{\chi}(A) - A \hat{\chi}(\nabla^2 \psi) + \rho_s^2 \langle v_y \rangle'' A \partial_y \psi + \langle v_y \rangle A \partial_y \psi + v^* A \partial_y \psi, \quad (4)$$

respectively. Here, we define the differential operator $\hat{\chi} \equiv \rho_s^2 (\partial_t + \langle v_y \rangle \partial_y)$.

The flow evolution equation follows as

$$\frac{1}{\rho_s^4 \Omega_i^2} \partial_t \langle v_y \rangle = \partial_x^2 A \partial_y A + \partial_{xy} A \partial_x A + A^2 [\partial_x^2 \psi \partial_y \psi + \partial_{xy} \psi \partial_x \psi] + 2A \partial_x A \partial_x \psi \partial_y \psi - \frac{\mu}{\rho_s^2 \Omega_i^2} \langle v_y \rangle. \quad (5)$$

Equations (3)–(5) thus systematically describe the evolution of the amplitude, phase, and the flow, respectively. Note that the flow can evolve via amplitude inhomogeneity or phase curvature.

III. PHASE AND FLOW EVOLUTION

In this section, we explore coupled phase and flow evolution for the limit of a single wave with amplitude $A = \text{const}$. The purpose of considering this unusual limit is to isolate the role of phase curvature in the Reynolds force, so as to better understand the physics of phase dynamics. The physics of intensity ($\sim |A|^2$) inhomogeneity in flow generation has been well studied.^{16,17}

We focus on the terms $\sim A^2$ in Eq. (5). These capture wave interactions which drive the flow. The second term in the expression disappears once averaged, since $\partial_{xy}\psi\partial_x\psi = \frac{1}{2}\partial_y(\partial_x\psi)^2$, the average of which vanishes. However, the first term clearly indicates the possibility of driving zonal flows through the radial curvature of the phase (i.e., $\partial_x^2\psi \neq 0$), even for homogeneous intensity (i.e., $\nabla I = \nabla(A^2) = 0$).¹¹

Alternatively, if one were to represent the drift wave by the usual eikonal form, such that $\tilde{\phi} = Ae^{i(\mathbf{k}\cdot\mathbf{x}-\omega t)}$, where $\mathbf{k} = (k_x, k_y) \sim (\partial_x\psi, \partial_y\psi)$ and $\mathbf{x} = (x, y)$, the Reynolds stress $\langle\partial_y\tilde{\phi}\partial_x\tilde{\phi}\rangle$ would then reduce to $k_x k_y A^2$, for constant amplitude. By going beyond lowest order eikonal theory, we see that the radial derivative of the stress also acts upon the cross phase $k_x k_y$. The radial gradient of the Reynolds stress $\partial_x\langle\partial_y\tilde{\phi}\partial_x\tilde{\phi}\rangle$ may thus be expressed as $k_x k_y \partial_x(A^2) + A^2 \partial_x(k_x k_y)$. The first term represents the usual mechanism for driving zonal flows through amplitude modulation. The second term shows that the gradient of the radial wavenumber ($\partial_x k_x$), i.e., the ‘‘phase curvature,’’ may also drive the zonal flow, even in the absence of inhomogeneous intensity. The latter mechanism of zonal flow generation and its effect on the underlying amplitude and flow structure of the DW-ZF system is our primary focus in this paper. We pursue this end by taking A as constant, hereafter.

We demonstrate zonal flow production through phase, rather than amplitude, modulation, by the use of WKB. We thus drop all terms of $O(\nabla A)$ and higher, thus effectively limiting the analysis to the case of homogeneous amplitude. Then, our system reduces to

$$0 = \nabla^2\psi \hat{\chi}(\psi) + 2\nabla\psi \cdot \hat{\chi}(\nabla\psi), \quad (6)$$

$$0 = \partial_t\psi + (\nabla\psi)^2 \hat{\chi}(\psi) - \hat{\chi}(\nabla^2\psi) + \rho_s^2 \langle v_y \rangle'' \partial_y\psi + \langle v_y \rangle \partial_y\psi + v^* \partial_y\psi, \quad (7)$$

$$\frac{1}{\rho_s^4 \Omega_i^2} \partial_t \langle v_y \rangle = A^2 \partial_x^2 \psi \partial_y \psi + A^2 \partial_{xy} \psi \partial_x \psi - \frac{\mu}{\rho_s^4 \Omega_i^2} \langle v_y \rangle. \quad (8)$$

The residue of the amplitude evolution Eq. (6) acts as a constraint on the system. The phase field and flow evolution are given by Eqs. (7) and (8). Zonal flow generation through phase curvature can now be seen explicitly through the first term on the right hand side of Eq. (8).

An important question is how to reconcile constant amplitude with energetics. In the course of DW-ZF energy exchange, drift wave instabilities lead to the formation of eddies, which drive transport and flows. The flows then feed back on the instability, shearing the eddies and so causing refraction and changes in k_r , in the process.^{18–20} This ultimately leads to the transfer of eddy energy to the flow. Specifically, the fluctuation energy evolves according to²¹

$$\begin{aligned} \frac{d\langle \varepsilon \rangle}{dt} &= \frac{1}{2} \langle \partial_t(\tilde{\phi}^2 + \rho_s^2(\nabla\tilde{\phi})^2) \rangle \\ &= \left\langle \tilde{\phi} \left[\partial_t \tilde{\phi} - \rho_s^2 \partial_t \nabla^2 \tilde{\phi} \right] \right\rangle, \end{aligned} \quad (9)$$

where we have performed an integration by parts (assuming boundary terms vanish) to obtain Eq. (9). Substituting into the Hasegawa-Mima Eq. (1) and exploiting periodicity in \hat{y} , we see that

$$\begin{aligned} \frac{d\langle \varepsilon \rangle}{dt} &= \langle v_y \rangle \langle \tilde{\phi} \partial_y \nabla^2 \tilde{\phi} \rangle = -\langle v_y \rangle A^2 \langle \partial_x(\partial_x\psi \partial_y\psi) \rangle \\ &= -\langle v_y \rangle A^2 \langle \partial_x^2 \psi \partial_y \psi \rangle. \end{aligned} \quad (10)$$

Here, we consider a closed system, and so we may drop the boundary terms for the evolution of the fluctuation energy. Note that fluctuation energy evolves due to phase-curvature-driven Reynolds force, even for the case of constant amplitude.

The energy for the flow evolves as

$$\begin{aligned} \frac{d\langle E_{ZF} \rangle}{dt} &= \frac{1}{\rho_s^4 \Omega_i^2} \langle v_y \rangle \partial_t \langle v_y \rangle \\ &= \langle v_y \rangle A^2 \langle \partial_x^2 \psi \partial_y \psi \rangle - \frac{\mu}{\rho_s^4 \Omega_i^2} \langle v_y \rangle^2. \end{aligned} \quad (11)$$

The evolution of the total energy of the DW-ZF system, then, is given by

$$\begin{aligned} \frac{d\langle E_{tot} \rangle}{dt} &= \frac{d\langle \varepsilon \rangle}{dt} + \frac{d\langle E_{ZF} \rangle}{dt} \\ &= -\frac{\mu}{\rho_s^4 \Omega_i^2} \langle v_y \rangle^2. \end{aligned} \quad (12)$$

We see that energy is thus conserved in the overall DW-ZF system at constant A , up to damping and boundary flux. In this model with constant intensity, ∇k_r is responsible for the energy exchange between the fluctuation and the flow. Refraction here works via phase curvature (i.e., $\partial_x^2\psi \neq 0$). Sites of the steepest gradient in the radial wavenumber contribute the most energy flux (to large scale), indicating that these sites are where flow generation is most active.

To determine the evolution of the mean phase field and flow, we now proceed to eliminate the fast variation of the phase. Specifically, we write the phase as an initial monochromatic plane wave, with a fast dependence on \hat{y} , plus a slower function Θ , such that

$$\psi = k_y y - \omega_{k_y} t + \Theta(x, y, t), \quad (13)$$

with an eigenfrequency which varies slowly (on mesoscales) in space and time,

$$\omega_{k_y} = \frac{v^* k_y}{1 + \rho_s^2 k_y^2} + k_y \langle v_y \rangle. \quad (14)$$

By construction, then, $k_y \gg \partial_y \Theta$ and $\omega_{k_y} \gg \partial_t \Theta$. Furthermore, Θ varies in x such that $\rho_s^2 \langle v_y \rangle \partial_y \nabla^2 \Theta \simeq 0$ and $\rho_s^2 \partial_t \nabla^2 \Theta \simeq \rho_s^2 \partial_t \partial_{xx} \Theta$. The evolution of the phase (7) then follows as

$$\partial_t(\Theta - \rho_s^2 \partial_x^2 \Theta) = \rho_s^2 \frac{v^* k_y}{1 + \rho_s^2 k_y^2} (\partial_x \Theta)^2 - \rho_s^2 k_y \langle v_y \rangle''. \quad (15)$$

The second term on the left hand side represents the dispersion of the phase. The first term on the right hand side represents nonlinear phase interaction due to phase steepening. The last term describes frequency detuning by the flow curvature. It is evident that the phase dynamics are governed by the competition between the nonlinear evolution of the phase, through gradient steepening $(\partial_x \Theta)^2$ and dispersion $\partial_t \partial_x^2 \Theta$. Such a balance is characteristic of solitary wave formation.²²

Likewise, when the flow equation (8) is averaged, the second term on its right hand side, $\partial_{xy}\psi \partial_x\psi$, can be dropped. The flow evolution equation then reduces to

$$\frac{1}{\rho_s^4 \Omega_i^2} \partial_t \langle v_y \rangle = A^2 k_y \partial_x^2 \Theta - \frac{\mu}{\rho_s^4 \Omega_i^2} \langle v_y \rangle. \quad (16)$$

Thus, our reduced phase-flow system is described by Eqs. (15) and (16).

IV. PHASE SLIPS AND SHEAR LAYERS

For simplicity, and to obtain an analytical solution to the reduced phase-flow system, we consider the case of vanishing damping. As will be seen below, taking $\mu \rightarrow 0$ leads us to propagating zonal shear layer solutions, which balance ZF growth with the movement of the shear layer through the system.

In light of the above discussion, we look for solutions in the moving frame propagating at speed c , i.e., of the form $\Theta(x - ct)$. We thus transform the temporal derivative according to $\partial_t \rightarrow -c\partial_x$. Then, Eq. (16) can be directly integrated to get

$$\langle v_y \rangle = -\frac{A^2 k_y}{c} \partial_x \Theta + \frac{\alpha}{c}, \tag{17}$$

where α is an integration constant and $\rho_s^2 \Omega_i$ has been absorbed into A for simplicity of notation. It is evident that the flow structure, scale, and evolution are thus set by the structure of the phase gradient.

Substituting Eq. (17) back into Eq. (15), then multiplying both sides of the equation by Θ'' , and integrating once give

$$-\frac{c^2}{2} f'^2 + \frac{c^2 \rho_s^2 - \rho_s^2 k_y^2 A^2}{2} (f')^2 = \frac{1}{3} \frac{\rho_s^2 v^* k_y c}{1 + \rho_s^2 k_y^2} f^3 + \beta. \tag{18}$$

Here $f \equiv \Theta'$ and β is an integration constant, as well. Thus, the equation for the phase gradient is given by

$$x + x_0 = \int \frac{df}{Q(f, c)^{\frac{1}{2}}}, \tag{19}$$

where

$$Q(f, c) \equiv (f')^2 = \frac{2}{\rho_s^2} \frac{1}{c^2 - k_y^2 A^2} \left(\frac{1}{3} \frac{\rho_s^2 v^* k_y c}{1 + \rho_s^2 k_y^2} f^3 + \frac{c^2}{2} f^2 + \beta \right). \tag{20}$$

Since k_{yA} has units of velocity, we recognize it as the radial $\mathbf{E} \times \mathbf{B}$ velocity fluctuation.

For $\beta = 0$, (19) admits the exact solution

$$\Theta' = -\frac{3c(1 + \rho_s^2 k_y^2)}{2\rho_s^2 v^* k_y} \operatorname{sech}^2 \left(\frac{c}{2\rho_s} \frac{x + x_0}{\sqrt{c^2 - k_y^2 A^2}} \right). \tag{21}$$

The possible resonance at $c = k_y A$ arises from the balance between dispersion and the flow curvature. The waves sharpen approaching this limit. Thus, the flow there is more strongly driven. The solution suggests a critical Mach number $M_c = c/k_y A$, with the speed-amplitude relation $M > 1$. Figure 1(a) gives a sketch of a propagating localized shear layer. Note the dipolar shear and the pattern propagation at c . Figure 1(b) shows the flow $\langle v_y(x) \rangle$. This has the form of a localized jet.

The spatiotemporal structure of the phase gradient suggests a dynamic realization of the concept of a phase slip.⁶ Indeed, integrating Eq. (21) once more, we get

$$\Theta = -\frac{3(1 + \rho_s^2 k_y^2) \sqrt{c^2 - k_y^2 A^2}}{\rho_s k_y v^*} \tanh \left(\frac{c}{2\rho_s} \frac{x + x_0}{\sqrt{c^2 - k_y^2 A^2}} \right) + \Theta_0. \tag{22}$$

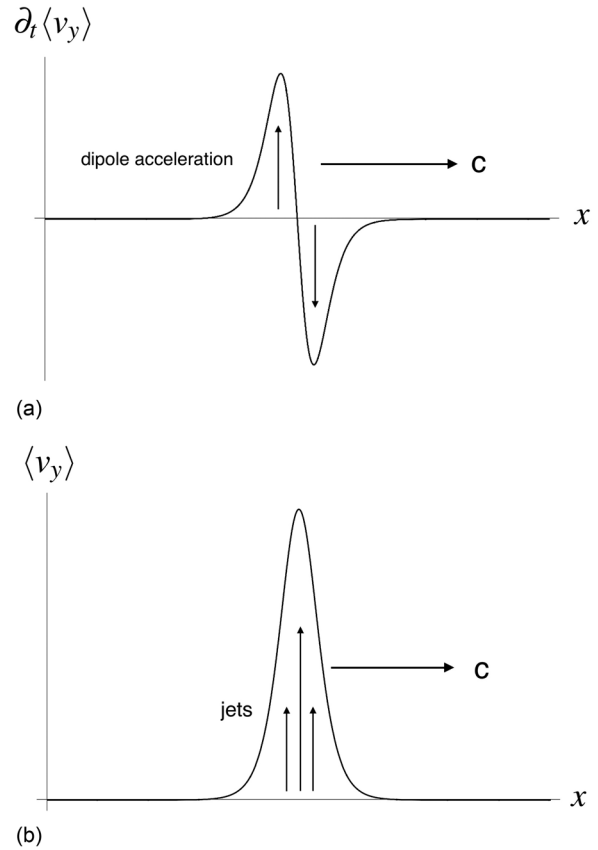


FIG. 1. Top (a): zonal flow evolution through the phase curvature. Bottom (b): zonal shear flow pulses induced by the slip.

Equation (22), which predicts a tanh profile for the phase, implies that at sites of intense zonal shearing, the phase “slips,” initiating refraction and zonal flow generation through phase curvature (Fig. 1). Figure 2 gives a sketch of a phase bore pattern, as suggested by Eq. (22). Note phase variation is isolated in a narrow layer, corresponding to the position of the velocity jet. The bore propagates across the system. Since

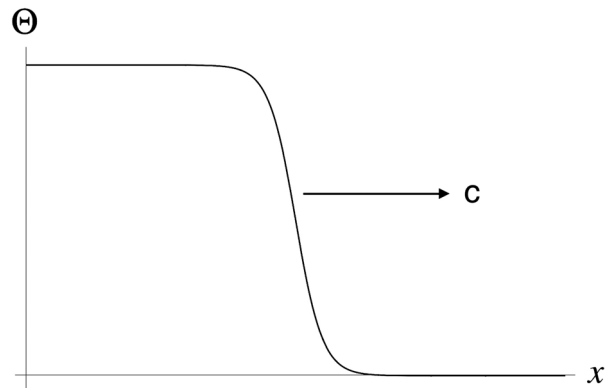


FIG. 2. Phase bore or slip propagating across the system.

the DW fluctuation is invariant under $\psi \rightarrow -\psi$, the phase can slip in both directions. As $M \rightarrow 1$, the width of the pattern decreases and thus the slip sharpens. However, the amplitude of the slip is more strongly attenuated approaching resonance.

The analytical solution for the phase gradient (21) defines the structure and scales of the zonal flow. The magnitude of the emergent shear flow pulse is set by $3A^2(1 + \rho_s^2 k_y^2)/2\rho_s v^*$ for $\alpha = 0$. The characteristic width of the pulse is given by $2\rho_s \sqrt{c^2 - k_y^2 A^2}/c$. The pulse is sharper near resonance.

We now address the stability of the phase and flow solutions by considering a ZF-based state (i.e., no streamers). In this state, we restrict the amplitude to be a function only of x . Thus, along the surfaces of constant amplitude at a particular constant radius, the dynamics of the phase are set by $k_y y$. Thus, by transforming $\nabla A \rightarrow \partial_x A$, our coupled amplitude-phase-flow equations (3)–(5) reduce to

$$\begin{aligned} \partial_t \left[(1 + \rho_s^2 [(\partial_x \Theta)^2 + k_y^2]) A - \rho_s^2 \partial_x^2 A \right] \\ = \frac{v^* \rho_s^2 k_y}{1 + \rho_s^2 k_y^2} (2 \partial_x \Theta \partial_x A + A \partial_x^2 \Theta), \end{aligned} \quad (23)$$

$$\begin{aligned} A \partial_t \Theta - \rho_s^2 \partial_t [(A \partial_x^2 \Theta) + 2(\partial_x \Theta \partial_x A)] \\ = \frac{v^* \rho_s^2 k_y}{1 + \rho_s^2 k_y^2} (A (\partial_x \Theta)^2 - \partial_x^2 A) - \rho_s^2 k_y A \langle v_y \rangle'', \end{aligned} \quad (24)$$

$$\frac{1}{\rho_s^4 \Omega_i^2} \partial_t \langle v_y \rangle = k_y A^2 \partial_x^2 \Theta + 2k_y A (\partial_x \Theta \partial_x A) - \frac{\mu}{\rho_s^4 \Omega_i^2} \langle v_y \rangle. \quad (25)$$

We consider a small radially varying perturbation of the homogeneous amplitude state while linearizing, i.e.,

$$A = A_0 + \varepsilon A_1(x, t).$$

Likewise, the flow and phase are perturbed to the same order,

$$\begin{aligned} \langle v_y \rangle &= \langle v_y \rangle_0(x, t) + \varepsilon \langle v_y \rangle_1(x, t) \\ \Theta &= \Theta_0(x, t) + \varepsilon \Theta_1(x, t). \end{aligned}$$

Here, our base states for the flow and phase are given by Eqs. (17) and (22), respectively. Since the base states are traveling waves, we transform the above equations from the stationary frame x to the moving frame $x - ct$ for perturbative analysis. Thus, we take $\partial_x \rightarrow \partial_x$ and $\partial_t \rightarrow -c\partial_x + \partial_t$.

A numerical calculation is used to demonstrate the stability of the perturbations (Fig. 3). Parameters are chosen to correspond to those of CSDX (Controlled Shear Decorrelation Experiment) plasma,²³ with vanishing damping and base amplitude $A_0 = 1$. Here, $c = 21$ and $k_y = 20$. Spatial discretization is employed through finite-difference methods. The amplitude perturbation is initialized at 10^{-5} at $x = 0$, with a Dirichlet boundary condition imposed at the right endpoint ($A_1(x_f, t) = 0$) and Neumann boundary conditions at both endpoints ($\partial_x A_1|_{x=0, x_f} = 0$). Here, x_f corresponds to the radial edge of the plasma. We impose both Dirichlet ($\Theta_1(x_f, t) = \langle v_y(x_f, t) \rangle_1 = 0$) and Neumann boundary conditions ($\partial_x \Theta_1|_{x=0, x_f} = \partial_x \langle v_y \rangle_1|_{x=0} = 0$) on the phase and flow perturbations without initial perturbations [$\Theta_1(x, 0) = \langle v_y(x, 0) \rangle_1 = 0$]. Note that after a short period of transient growth, the perturbations decay to zero, indicating stability.

V. DISCUSSION AND CONCLUSION

In this paper, we have studied how phase dynamics—and, in particular, phase curvature—affect zonal flow evolution. To isolate the effects of phase curvature, we start from a base state with constant drift wave amplitude. This eliminates intensity profile effects. The principal results of this paper are as follows:

- (i) We derived a coupled system of equations for wave phase, amplitude, and zonal flow. This system is simplified for a single wave, with spatiotemporally constant amplitude. This isolates the effect of the phase curvature on the flow generation process.
- (ii) The quasilinear phase-flow equations are solved analytically. Radially propagating solutions of the form $\Theta(x - ct)$, $\langle v_y(x - ct) \rangle$ are obtained. These novel examples of zonal shear layer structures are formed by the balance of phase steepening and dispersion and so resemble collisionless phase shocks or solitons.
- (iii) The results realize the prediction that phase curvature can generate shear flows, which regulate drift wave turbulence.
- (iv) The shear layers induce jumps or slips in the phase. These resemble propagating bores. Thus, stress-driven shear layers constitute a concrete realization of the concept of a phase slip.
- (v) We find that the phase-flow solutions obtained here are linearly stable.
- (vi) The implications of the results obtained for this simple model for phase turbulence are discussed in detail.

More generally, we see the cross phase $\cos \Phi = \langle \tilde{v}_r \cdot \tilde{v}_\theta \rangle / |\tilde{v}_r| |\tilde{v}_\theta|$ is critical to evolution of the Reynolds stress and thus is a key to self-regulation, as it includes the phase curvature effect. In

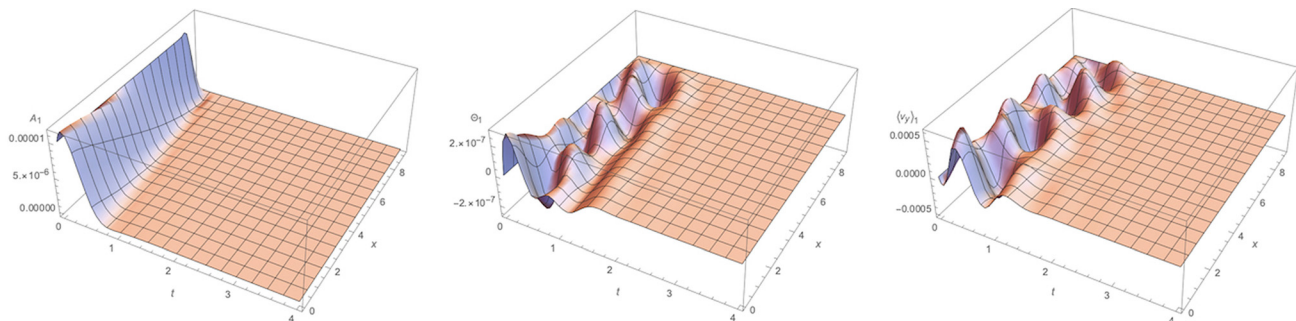


FIG. 3. Left-to-right shows amplitude, phase, and flow perturbations in x and t . Note that a finite amplitude state is initialized but, after transient growth, decays to zero, indicating the structure is stable.

particular, nonzero phase derivative, $\partial_x \psi = k_x \neq 0$, is required for a nonzero Reynolds stress. In general, anisotropy of \tilde{v}_x, \tilde{v}_y is required for nonzero Reynolds stress. For negligible amplitude inhomogeneity, radial variation of k_x (i.e., phase curvature $\partial_x^2 \psi \neq 0$) is required for a nonzero Reynolds force. This can directly drive zonal flow evolution through k_r inhomogeneity, even in the absence of intensity inhomogeneity. Note that either amplitude inhomogeneity or k_x inhomogeneity is required for a finite Reynolds force, as shown in Fig. 4. Phase curvature initiates a new feedback loop between phase and flow, causing the generation of nonlinear structures in the phase field—in particular, the birth of a stable, propagating phase bore. The bore induces a burst of intense evolution of k_r , causing a surge of energy transfer from drift waves to the flows. This burst in turn generates a propagating shear flow pulse. Both amplitude inhomogeneity and phase inhomogeneity contribute to the Reynolds force, which ultimately drives zonal flow. The two inhomogeneities each define a feedback channel connecting fluctuations and flow (Fig. 4). This channel is complementary to the well known amplitude modulation channel.

This paper does not address the state of “phase turbulence,” where many interacting modes produce an ensemble of phase bores, associated with shear layers. The system presented here can be generalized straightforwardly to realize a quasilinear theory of phase-flow turbulence, in which the slow phase $\Theta_{k_y}(x, t)$ and the flow $\langle v_y(x, t) \rangle$ fields evolve. In this restricted model, the intensities of the various modes ($\sim |A_{k_y}|^2$) are constant. Of course, the total phases ψ_{k_y} are given by $\psi_{k_y} = k_y y - \omega_{k_y} t + \Theta_{k_y}(x, t)$. The quasilinear equations then become

$$\partial_t(\Theta_{k_y} - \rho_s^2 \partial_x^2 \Theta_{k_y}) = \rho_s^2 \frac{v^* k_y}{1 + \rho_s^2 k_y^2} (\partial_x \Theta_{k_y})^2 - \rho_s^2 k_y \langle v_y \rangle'' \quad (26)$$

$$\frac{1}{\rho_s^4 \Omega_i^2} \partial_t \langle v_y \rangle = \sum_{k_y} |A_{k_y}|^2 k_y \partial_x^2 \Theta_{k_y} - \frac{\mu}{\rho_s^4 \Omega_i^2} \langle v_y \rangle \quad (27)$$

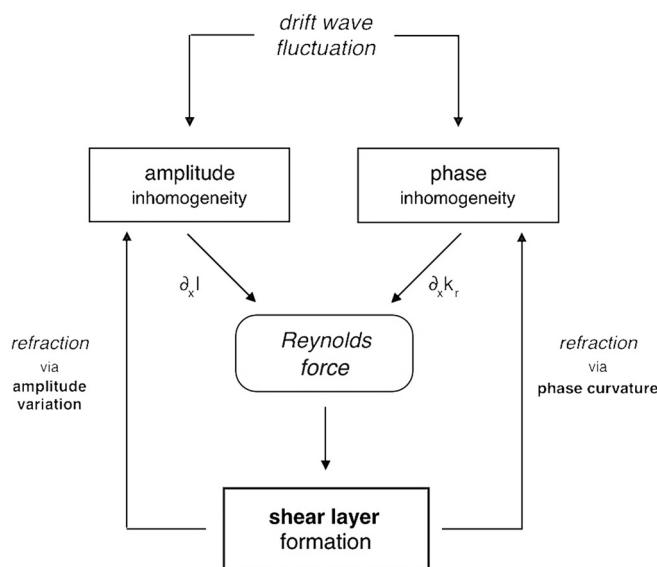


FIG. 4. Flow chart illustrating mechanisms of zonal flow generation and its feedback on the drift wave fluctuations, via either amplitude or phase inhomogeneity.

Thus, the flow field is produced by a sum of the phase curvatures, weighted by the modal intensities $|A_{k_y}|^2$. Self-interactions can drive resonant contributions to the phase equation (via $\langle v_y \rangle''$), as discussed above. Interactions with other modes produce nonresonant phase perturbations. Thus, in this model, the state of phase turbulence will consist of an ensemble of propagating phase slips or bores. Each bore is associated with a propagating zonal shear layer. Of course, the phase bores will also feed back on instability via the effects of the associated nonlinear frequency shift of the deviation of the wave frequency from the diamagnetic frequency (i.e., $\omega - \omega_e^*$).

To progress beyond mean field theory, the effects of mode-mode interaction on phase evolution must be addressed. One must consider the evolution of amplitude, phase, and flow, including instability processes. This requires extension to the Hasegawa-Wakatani model.²⁴ These analyses are beyond the scope of this paper. Other questions for future study include phase evolution in streamers, Kelvin-Helmholtz instabilities of the flow,²⁵ as well as boundary effects.

Finally, we suggest that a phase bore could be the leading edge of an avalanche.^{26–29} A phase slip which increases $\omega^* - \omega$ would trigger a burst of stronger transport and so initiate a propagating mixing and relaxation event—in other words, an avalanche.

ACKNOWLEDGMENTS

We thank Zhibin Guo for stimulating and insightful conversations on phase dynamics and Guilhem Dif-Pradalier for interesting conversations on bores and avalanches. We also thank participants in the 2017 and 2019 Festival de Théorie for stimulating discussions. This research was supported by the U.S. Department of Energy, Office of Science, Office of Fusion Energy Sciences under Award No. DE-FG02-04ER54738.

REFERENCES

- ¹J. W. Conner and H. R. Wilson, *Plasma Phys. Controlled Fusion* **36**, 719 (1994).
- ²R. Sagdeev and A. Galeev, *Nonlinear Plasma Theory*, Frontiers in Physics (W. A. Benjamin, 1969).
- ³H. Biglari, P. H. Diamond, and P. W. Terry, *Phys. Fluids B* **2**(1), 1–4 (1990).
- ⁴Z. B. Guo and P. H. Diamond, *Phys. Rev. Lett.* **114**, 145002 (2015).
- ⁵T. H. Dupree, *Phys. Fluids* **9**, 1773 (1966).
- ⁶A. Pikovsky, M. Rosenblum, and J. Kurths, *Synchronization: A Universal Concept in Nonlinear Sciences*, Cambridge Nonlinear Science Series (Cambridge University Press, 2001).
- ⁷P. Manneville, in *Dissipative Structures and Weak Turbulence* (Academic Press, Boston, 1990) pp. 369–418.
- ⁸D. Y. Manin, *Phys. Fluids A* **4**, 1715 (1992).
- ⁹R. Adler, *Proc. IRE* **34**, 351 (1946).
- ¹⁰P. H. Diamond, S.-I. Itoh, K. Itoh, and T. S. Hahm, *Plasma Phys. Controlled Fusion* **47**, R35 (2005).
- ¹¹Z. B. Guo and P. H. Diamond, *Phys. Rev. Lett.* **117**, 125002 (2016).
- ¹²A. Hasegawa and K. Mima, *Phys. Fluids* **21**, 87 (1978).
- ¹³R. Sagdeev, *Rev. Plasma Phys.* **4**, 23 (1966).
- ¹⁴A. Hasegawa, C. G. MacLennan, and Y. Kodama, *Phys. Fluids* **22**, 2122 (1979).
- ¹⁵R. Sagdeev, V. Shapiro, and V. Shevchenko, *Fiz. Plazmy* **4**, 551–559 (1978).
- ¹⁶Ö. D. Gürçan and P. H. Diamond, *J. Phys. A* **48**, 293001 (2015).
- ¹⁷L. Chen, Z. Lin, and R. White, *Phys. Plasmas* **7**, 3129 (2000).
- ¹⁸P. H. Diamond, Y.-M. Liang, B. A. Carreras, and P. W. Terry, *Phys. Rev. Lett.* **72**, 2565 (1994).

- ¹⁹P. Manz, M. Ramisch, and U. Stroth, *Phys. Rev. Lett.* **103**, 165004 (2009).
- ²⁰Z. Lin, T. S. Hahm, W. W. Lee, W. M. Tang, and R. B. White, *Science* **281**, 1835 (1998).
- ²¹P. H. Diamond, A. Hasegawa, and K. Mima, *Plasma Phys. Controlled Fusion* **53**, 124001 (2011).
- ²²E. Lifshitz and L. Pitaevskii, in *Physical Kinetics*, edited by E. Lifshitz and L. Pitaevskii (Butterworth-Heinemann, Oxford, 1981) pp. 115–167.
- ²³S. C. Thakur, C. Brandt, L. Cui, J. J. Gosselin, A. D. Light, and G. R. Tynan, *Plasma Sources Sci. Technol.* **23**, 044006 (2014).
- ²⁴M. Wakatani and A. Hasegawa, *Phys. Fluids* **27**, 611 (1984).
- ²⁵E.-J. Kim and P. H. Diamond, *Phys. Plasmas* **10**, 1698 (2003).
- ²⁶P. Bak, C. Tang, and K. Wiesenfeld, *Phys. Rev. Lett.* **59**, 381 (1987).
- ²⁷P. H. Diamond and T. S. Hahm, *Phys. Plasmas* **2**, 3640 (1995).
- ²⁸T. S. Hahm and P. H. Diamond, *J. Korean Phys. Soc.* **73**, 747 (2018).
- ²⁹G. Dif-Pradalier, V. Grandgirard, Y. Sarazin, X. Garbet, and P. Ghendrih, *Phys. Rev. Lett.* **103**, 065002 (2009).